

Application of microseismic monitoring technology in the prevention and control of dynamic disasters in the excavation face of Liyazhuang Mine

Yuheng Che ^{1,2,*}

¹State Key Laboratory of the Gas Disaster Detecting, Preventing and Emergency Controlling, Chongqing, China

²Chongqing Research Institute of China Coal Technology and Engineering Group Corp., Chongqing, China

*Corresponding author Yuheng Che

Abstract

The excavation working face 2-228 in Liyazhuang Mining Area 2 of Huozhou Coal and Electricity Group is a key prevention and control area for rock burst. During the production period of the mine and when the working face is under pressure, the probability of corresponding strong mining earthquakes is relatively high, and it is easy to cause accidents of roof falling and falling, causing injuries to people. Taking the 2-228 working face of Liyazhuang coal mine as the research object, the detected microseismic raw signals were subjected to window Fourier transform to analyze the microseismic spectra of different energy levels. The research results indicate that the waveform morphology and spectrum corresponding to signals at different energy levels have different characteristics. High amplitude, low and concentrated main frequency, long signal duration, obvious coda development compared to the first wave, and slow attenuation rate are typical characteristics of strong mining earthquakes. As the energy of the mining earthquake decreases, the attenuation rate of the vibration gradually increases, the signal duration shortens, the development of the first wave begins to be obvious, and the velocity amplitude decreases with phase strain. But the rate of amplitude reduction gradually slows down, and the main frequency gradually develops from concentration to diffusion, while the influence of frequency distribution range is not significant.

Keywords

Dynamic disaster; Microseismic monitoring technology; Excavation working face; Energy level; Spectrum analysis.

1. Introduction

The Liyazhuang coal mine of Huozhou Coal and Electricity Group is located on the northern edge of the Linfen Basin in southern Shanxi Province, with a designed production capacity of 1.5 million tons/year. It is a high gas mine. After entering the deep part of the second mining area, due to the influence of hilly terrain, the surface rises, and the mining depth reaches over 600m. The mine pressure significantly increases, manifested by large deformation of the roadway, severe floor heave, and frequent coal explosions. The 2-228 excavation face currently being prepared is a mined out isolated island working face on both sides of the upper and lower sections. Affected by factors such as plateau rock stress, mining concentrated stress, and gas, coal guns are frequent during the excavation period, leading to severe top drilling and pinching during drilling, as well as frequent borehole spraying, posing a serious threat to underground

safety production. According to the analysis of the current mining technical conditions, the hazard that causes the dynamic phenomenon of the mine has multiple factors: the energy gathered in the coal seam due to high stress, the huge elastic energy gathered in the multi-layer hard roof, and the internal energy of gas can all become the energy source of the dynamic phenomenon of the mine.

At present, emerging geophysical methods such as acoustic emission method, electromagnetic radiation method, and microseism [1-5] have been rapidly developed and applied to the coal mining industry. Among them, microseism is widely used in rock burst and outburst mines due to its high sensitivity, safety, and reliability. Especially in recent years, the application of microseismic monitoring technology in mines has developed rapidly and has great practical significance [6-9]. Therefore, based on the above analysis, taking the 2-228 excavation working face of Liyazhuang Coal Mine of Shanxi Huozhou Coal and Electricity Group Company as the research object, the SOS microseismic monitoring system is used to remotely, real-time, dynamically, and automatically monitor the seismic signals of the 2-228 working face of Liyazhuang Coal Mine, and to develop corresponding prediction and prevention methods. This also provides useful reference for other mining areas and mines with similar conditions in the group company.

2. Implementation of microseismic monitoring on-site

During the period from June 1 to June 30, 2011, there were three pressure surges in Liyazhuang 2-228 working face. Among them, June 5 was the first pressure surge, June 13 was the second pressure surge, and June 23 was the third pressure surge. The average pressure step distance of this working face is 31m, and the average maximum working resistance of the support is 35MPa. It can be inferred that the mining pressure of this working face is relatively high, and stress concentration is highly likely to cause dynamic phenomena such as impact ground pressure.

Liyazhuang Coal Mine has introduced the SOS microseismic monitoring system to remotely, real-time, dynamically, and automatically monitor the seismic signals of the mine, including rock burst. It accurately calculates the time, energy, and spatial coordinates of vibrations with energy greater than 100J and the occurrence of rock burst. The system consists of 1HZ-600HZ vibration recording performance, a geophone measurement probe with embedded signal output template, a central signal data receiver, a digital information recorder with signal monitoring and analysis template, and a central computer. The original microseismic signal is transformed into time-domain and frequency-domain through window Fourier transform, ultimately obtaining the energy magnitude and spectral characteristics of the microseismic signal.

The microseismic sensor measurement points should be uniformly arranged near the working face and form a network structure. The final measurement point layout plan is shown in Table 1. The DLM-2001 type detector probe is now selected, and the probe is fastened to the thread at the end of the anchor rod, with a metal steel pipe protective cover added. The output cable of the probe should be connected through the underground explosion-proof junction box.

Table 1 Layout plan of sensor measurement points

Number	Position	Coordinate		
		X	Y	Z
1	6022 air door to return air lane	37570606.00	4058645.00	266
2	Central substation of return air downhill in mining area 6	37569564.00	4059324.00	304
3	355 return air lane substation	37567261.00	4058164.00	363.8

	2			
4	At the return air roadway at the bottom of the main shaft	37566700.00	4057296.00	321.5
5	At 2281 alley of returning air down mountain in mining area 2	37568281.00	4056688.00	228
6	2281 lane in mining area 2	37568599.00	4057151.00	235
7	2282 lane in mining area 2	37568699.00	4057071.00	216
8	At 2282 alleys in the return air downhill of the second mining area	37568455.00	4056627.00	225
9	Bottom of return air downhill in mining area 2	37568911.00	4056468.00	202
10	At the second mining area return air downhill and the second and fourth air distribution roadway	37567733.00	4056877.00	275
11	At the four mining area return air downhill and the second and fourth air distribution roadway	37568230.00	4057494.00	294.5

3. Microseismic spectrum analysis

During the one month period from June 1 to June 30, 2011, the microseismic monitoring system of the mine recorded that the energy of microseismic events was mainly concentrated between $10^2 \sim 10^5$ J. Each generated microseismic signal is received by multiple sensor measurement points. Due to the propagation distance of the vibration signal in the medium, the waveform, frequency band, and other characteristics of the signals monitored by sensor measurement points at different distances from the source are different. Due to the length, only the waveform and spectral characteristics of the signals received by the sensor measurement points closest to the source are analyzed.

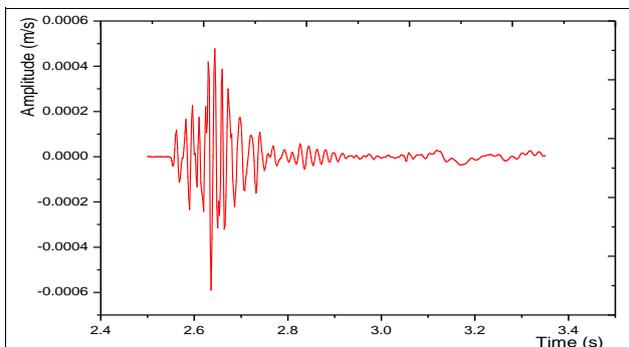
3.1. Waveform and spectral characteristics of microseisms with energy above 10^4 J

On June 13, 2011, a vibration with an energy of 3.99×10^4 J was detected, where the source is relatively close to channel 6, is shown in Figure 1 for some waveforms and spectra of this channel. As shown in Figure 1 (a), for mining earthquakes of this energy level, the amplitude range of signal waveform vibration velocity is relatively large, mainly between $0.6 \times 10^{-4} \sim 6.5 \times 10^{-4}$ m/s, the duration of microseismic signals ranges from 800 to 2000ms. From Figure 1 (b), it can be seen that the frequency band of microseismic signals is mainly between 0~200Hz, with a main frequency of 40~70Hz.

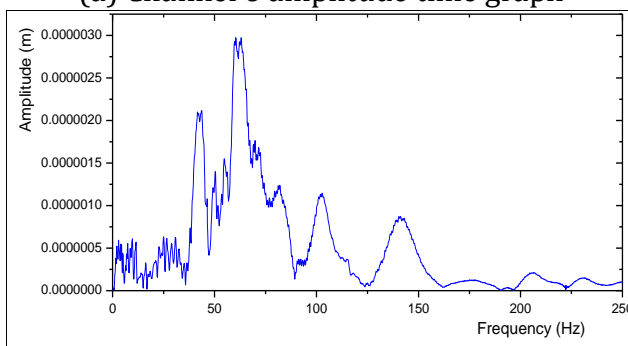
3.2. Waveform and spectral characteristics of microseisms with energy above 10^3 J

On June 6th, a vibration with an energy of 1.05×10^3 J was detected. And it is located closest to channel 6, and its partial waveform and spectrum are shown in Figure 2. As shown in Figure 2 (a), for mining earthquakes of this energy level, the amplitude range of signal waveform vibration velocity is relatively large, mainly between $0.2 \times 10^{-4} \sim 5.0 \times 10^{-4}$ m/s, the duration of microseismic signals becomes shorter, within the range of 600~1800ms. From Figure 2 (b), it can be seen that the frequency band distribution of microseismic signals ranges from 0 to

160Hz, with a wider main frequency and significantly lower frequencies, ranging from 10 to 75Hz. Combined with on-site production activities underground, microseismic signals with such waveform characteristics and vibration energy of around 1000J are mostly caused by underground blasting.

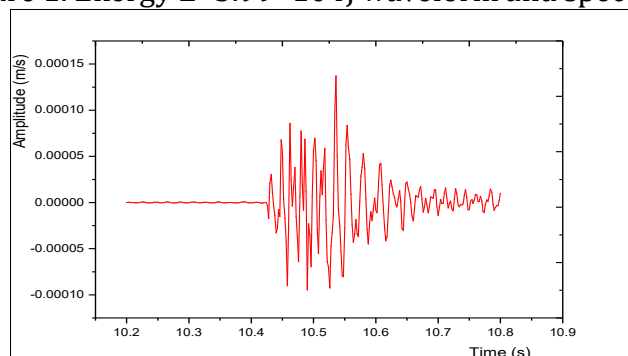


(a) Channel 6 amplitude time graph

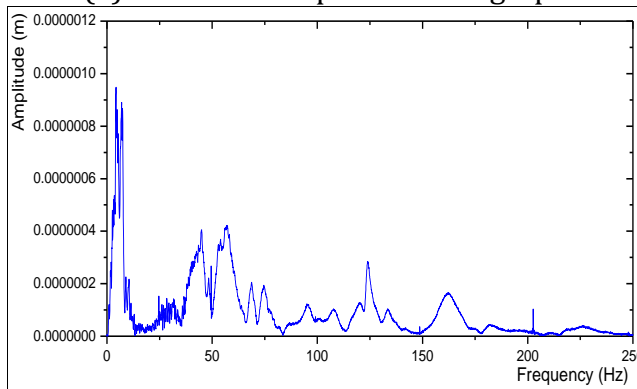


(b) Channel 6 amplitude frequency graph

Figure 1. Energy $E=3.99 \times 10^4$ J waveform and spectrum



(a) Channel 6 amplitude time graph

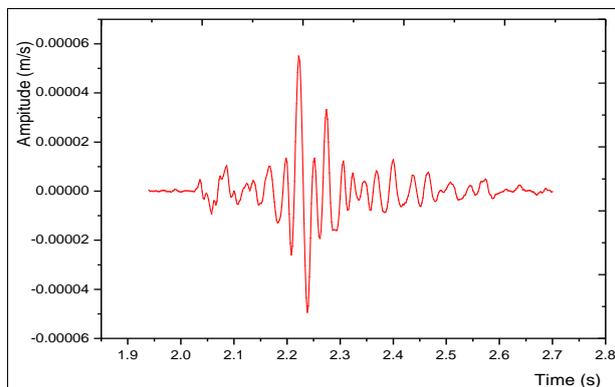


(b) Channel 6 amplitude frequency graph

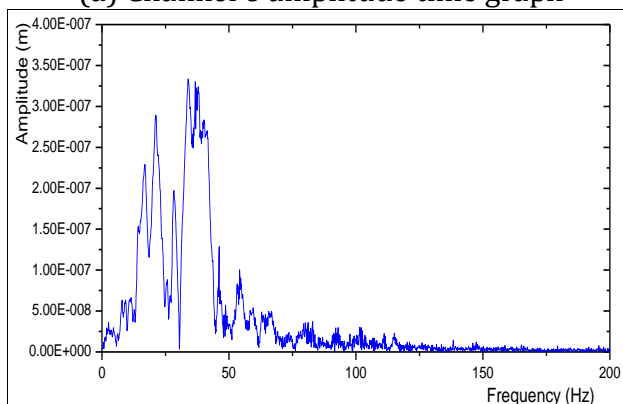
Figure 2. Energy $E=1.05 \times 10^3$ J waveform and spectrum

3.3. Waveform and spectral characteristics of microseisms with energy above 10^2J

On June 10th, a vibration with an energy of $8.71 \times 10^2\text{J}$ was detected. And it is located closest to channel 6, and its partial waveform and spectrum are shown in Figure 3. As shown in Figure 3 (a), the vibration velocity amplitude range of the mining earthquake signal waveform at this energy level has decreased, mainly between $0.2 \times 10^{-4} \sim 4.5 \times 10^{-4}\text{m/s}$, the signal duration is between $400 \sim 1200\text{ms}$ and decays quickly. From Figure 3 (b), it can be seen that the frequency band distribution of microseismic signals is between $0 \sim 160\text{Hz}$. Compared to high-energy signals, the main frequency band of low-energy vibrations is wider and more dispersed, ranging from 15 to 80Hz . Combined with on-site production activities underground, the vibrations with such waveform and energy characteristics and positioning results above the goaf are mostly caused by roof caving.



(a) Channel 6 amplitude time graph



(b) Channel 6 amplitude frequency graph

Figure 3. Energy $E=8.71 \times 10^2\text{J}$ waveform and spectrum

4. Conclusion

This article mainly uses the SOS microseismic monitoring system to remotely, real-time, dynamically, and automatically monitor the seismic signals of the 2-228 excavation face in Liyazhuang Coal Mine, and analyzes the microseismic spectra of different energy levels. And the waveform morphology and spectrum corresponding to signals at different energy levels have different characteristics. As the energy of the mining earthquake decreases, the attenuation rate of the vibration gradually becomes faster, the signal duration becomes shorter, and the development of the first wave begins to be obvious. The velocity amplitude decreases with the phase strain, but the rate of amplitude reduction gradually slows down. The main frequency gradually develops from concentration to diffusion, while the distribution range of signal frequency has little effect.

Acknowledgments

The study was supported by Major Independent Special Funding Projects of Chongqing Research Institute of China Coal Technology and Engineering Group Corp. (2021ZDZX07).

References

- [1] Kang Jiandong. Acoustic emission prediction technology for coal and gas outburst in the torsional structural belt of Donglin coal mine [J]. *Mining Safety and Environmental Protection*, 2013,40 (04): 53-55+58.
- [2] Li Hongde. Application of electromagnetic radiation method in predicting the risk of coal and gas outburst in Jiulishan mine [J]. *Mining Safety and Environmental Protection*, 2014,41 (03): 67-70.
- [3] Song Jie, Wang Jian, Liu Shang, et al. Prediction of rock burst using electromagnetic radiation method based on improved PSO-BP model [J]. *Coal Mine Safety*, 2019,50 (06): 205-208.
- [4] Liu Qiang, Wei Jinhong, Meng Qiaorong. Design and research of coal mine microseismic monitoring and positioning system [J]. *Coal Technology*, 2022,41 (08): 203-207.
- [5] Qin Min, Liu Chang, Wang Qian, et al. Analysis of Microseismic Monitoring and Warning Parameters for Ground Pressure Hazards in Mining Plants [J]. *Mining Research and Development*, 2022,42 (10): 180-186.
- [6] Mao Mingfa, Li Wu, Zhang Zeyu, et al. Construction and application of microseismic monitoring system for Huize lead-zinc mine [J]. *China Mining*, 2020,29 (S1): 169-175.
- [7] Zhang Guohua, Chen Dong, Lin Song. Study on time-frequency characteristics of microseismic signals and precursor characteristics of rock burst in Gengcun coal mine [J]. *Industrial and Mining Automation*, 2021,47 (12): 87-92+97.
- [8] Qin Kaifeng. Study on stability of surrounding rock of 3604 heading face based on microseismic monitoring technology [J]. *Shandong Coal Science and Technology*, 2023,41 (01): 168-170.
- [9] Long Long, Li Meng. Analysis of microseismic energy activity patterns in the 1012007 working face of Yuanzigou Coal Mine [J]. *Coal*, 2023,32 (02): 88-90+97.